SUPPORT TO OPERATIONAL HYDROLOGY AND WATER MANAGEMENT-SAF

FINNISH METEOROLOGICAL INSTITUTE

ROMANIA
NATIONAL METEOROLOGICAL ADMINISTRATION

Snow detection algorithm based on Meteosat-8 RGBHRV139i composite images and comparison with HSAF and LSA SAF snow recognition products

Simona Oancea
National Meteorological Administration, Romania

Pirkko Pylkko, Panu Lahtinen
Finnish Meteorological Institute

Visiting Scientist Report
30 September 2007

Acknowledgements

This research was done as a visiting scientist activity of Simona Oancea at the Finnish Meteorological Institute, from 1 February 2007 to 30 September 2007, in the context of SUPPORT TO OPERATIONAL HYDROLOGY AND WATER MANAGEMENT-SAF, EUMETSAT Program.

Abstract

Originally it was planned to test and compare all HSAF snow products. This turned out not to be feasible, because SWE, SCA and snow status products were last winter only in a very preliminary stage. Therefore the study concentrated only on snow recognition product and comparisons with HSAF and LSA SAF methods.

This report has the following structure:

Section 1

- **a preliminary snow detection algorithm has been developed using Meteosat-8 RGB 139i composite images. Meteosat-8 was used, because winter 2006/2007 Meteosat-9 was not yet operationally available. It was foreseen better to use Meteosat-8, which had stable behaviour and calibration. The Meteosat-8 images were received through the operational LRIT/HRIT-Kongsberg receiving station installed at the Finnish Meteorological Institute.**
  This preliminary algorithm has a tendency to underestimate the snow cover area a bit, but it is somewhat better in discriminating snow and clouds.

Section 2

- **a new algorithm has been created by adding MSG HRV channel to the visible channels VIS0.6 and NIR1.6 from the previous combination.**
  Algorithm at this stage can discriminate snow and clouds rather reliably. It has a tendency to underestimate snow covered area especially in the boreal forest during melting season.

Section 3

- **two different snow map comparisons have been performed. The first comparison has been done between RGBHRV139i snow cover maps and HSAF snow cover maps. The second comparison is between RGBHRV139i snow cover maps and LSA SAF snow cover maps (development version).**
  The RGBHRV139i snow cover maps have a tendency to mapping snow better than HSAF snow cover map but less than LSA SAF snow cover map specially in forested area (i.e., Finland).
  Also for both comparisons, there are differences at the edges of snow snow cover algorithm mapped more snow than others.

Table of Contents

Overview

The main topic of visiting scientist activity is
Modifying and testing of algorithms prototyped in Finland for Romania and other Central European countries

The objective of the work period, February 1, 2007- September 30, 2007, was to develop a *snow detection algorithm using Meteosat8 RGBHRV 139i composite images for the H-SAF geographical area.*
This algorithm is then used for comparison of the present HSAF baseline and LSA SAF development algorithms.

Section 1

1. RGB139i (VIS0.6, NIR1.6, IR10.8i) snow cover algorithm

Up-to-date information about surface snow cover over large areas can be obtained with remote sensing using the satellite images that are acquired at short time intervals. SEVIRI on board Meteosat Second Generation (MSG) can be used for this task: the high temporal frequency of 15 minutes makes it possible to detect all cloud-free situations and to monitor short-term changes in snow cover. It can also be used to detect the temporal behaviour of clouds, which helps to overcome a well-known problem in remote sensing of snow, namely the confusion of ice clouds with snow. Still, SEVIRI and MSG concept have two disadvantages for snow mapping: poor spatial resolution and very low viewing angle at high latitudes. This makes an extra challenge to the algorithm development.
In this section we present a preliminary snow mapping algorithm for SEVIRI that uses temporal information, in addition to spectral information.

1.1. Overview

The high potential of monitoring snow cover from space has been demonstrated in numerous studies using sensors operating in the reflective, thermal and microwave spectral domain. In the past, only polar-orbiting (low-frequency) satellite sensors had the required spectral or spatial resolution to accurately distinguish between snow cover and clouds. With the launch of the first MSG (Meteosat Second Generation) in 2002 (operational since 2004), geostationary satellite systems became feasible to address this sometimes difficult task. This sensor series offers high resolution, both in the spectral and temporal domain (covering the visible to thermal in 12 spectral bands every 15 minutes).

1.2. Source of data

Meteosat-8 satellite data was provided through the LRIT/HRIT-Kongsberg receiving station installed at Finnish Meteorological Institute. The satellite data used are provided in HDF5 format. These consist of raw digital counts, which need to be calibrated and converted into reflectance and brightness temperature.
An important feature of these HDF files is that the files are self-describing. By grouping related pieces of information together and forcing a certain file structure, it is easy for the users to make use of the data. We also applied a land/sea mask to the data for the study area which is available at the FMI server. For testing and validation we selected a 27 day period in March 2007 starting from March 12 to April 10 and usually we collected the images from 7:00 GMT to 16:00 GMT, sometimes until 18:00 GMT (1126 Meteosat-8 images).
Several days of this period (March 16, 17 and 18) are missing. During the selected period most of the mountainous regions of Europe were covered with snow. All the classes which are important for our preliminary snow algorithm (clouds with ice

particles, free surfaces, and snow cover surface) were all well illustrated into the selected satellite images.

1.3. Study area

The area of the study is Europe and defined the same way as for other HSAF snow products.

1.4. Method

Discrimination between clouds and sea ice or snow using spectral methods has been discussed by Romanov P. et al. in [13], Gesell in [4], Allen et al. in [1] and Hall et al. in [6]. Snow and clouds share some spectral characteristics.

The basic techniques used in our preliminary snow detection methodology are the threshold based criteria tests and we used a RGB combination instead of the classic channels.
The main steps of this algorithm are:

- RGB 139 (VIS0.6, NIR1.6, IR10.8) composition images method
- Snow pixel detection using the RGB threshold values test
- A cloud contamination removal method which consists of:
  - A standard deviation classification test
  - A test to remove residual Cirrus clouds
  - A temporal classification test
  - A spatial consistency test
- Snow composite product method

1.4.1. RGB 139i (VIS0.6, NIR1.6, IR10.8) composition images method.

RGB images offer the possibility to pack the information of more than 3 different images into a single image using colours. This enables the viewer to identify the main input signal, when the resulting colour shows a clear tendency to red, green or blue. More information about RGB tools is available on the EUMETSAT site, in [11].
For our aim we used RGB139i (VIS0.6, NIR1.6, IR10.8) images obtained by using the Meteosat-8 satellite. In this combination there are channels very sensitive to areas covered by the snow and ice and also to clouds that are mainly composed of ice particles (channel 3, i.e NIR1.6).
The use of the 1.6μm channel available from the AVHRR/3 instrument for accurate threshold test based classification of snow/clouds/clear pixels was thoroughly examined by Hyvarinen et. al in [7] studying the separation of snow covered surfaces from water clouds, cirrus clouds, sun-glint, water and land surfaces. Results showed that using the 0.6μm and 1.6μm channel it is possible to accurately separate snow from water clouds and clear surfaces.

The band IR10.8 was selected because it represents an atmospheric window, in which little of the emitted thermal radiation is absorbed by the atmosphere and this makes easier the recognition of cloud systems. The ,,i'' in RGB139i stands for

“inverted” and means that pixel values increase with the decreasing of temperature for infrared channel 9.

Visual discrimination between ice clouds and snow can be facilitated by making use of the RGB139i combination. In this combination, most image classes are clearly discernible from each other. Water clouds are yellowish in this plot, because they display high values in the first two components. Snow-free surfaces have intermediate near infrared reflectance (second component) and low values in the other components, and thus appear green. Snow appears as dark pink to magenta because it only has a high reflectance at 0.6 μm. Optically thin ice clouds (cirrus) tend to be blue and optically thick ice clouds are pink to magenta. Animated time series of this RGB combination show the spectral and the temporal component of every class mentioned above.

In order to obtain these RGB images a set of adjustments have to be done. These adjustements included:

– Extraction of the satellite data

in order to detect the snow area using this algorithm we have used the raw satellite data provided by the channels: VIS0.6, NIR1.6, IR10.8.

– Geometric coding

The latitude and longitude data (in degrees) in the satellite projection used for our interest area are available on the HDF5 format on the following ftp site:
ftp://gerb.oma.be/seviri/Geolocation

– Solar zenith angle calculations

Documentation to implement this step is provided by EUMETSAT in [5]
The use of at-satellite reflectance collected at very low solar elevation angles is complicated because of an increasing influence of atmospheric effects and cloud shadows. To reduce the effect of these factors in our snow detection algorithm we limit the allowable measurement of solar zenith angle lower or equal to 80^0.

– Radiometric calibration

The radiometric conversion procedure was compiled from the EUMETSAT website [8]

– RGB combination images product

All the processing stages were written in the IDL language and run on the FMI server.

This routine generates two files:

- the RGB image file
- the quality - flag file for every RGB image.

We have noticed that sometimes the reflectance is more than 1. Sometimes clouds, ice/snow, water surfaces can cause specular reflection. In that case the reflection coefficients can become higher than 1.

1.4.2. RGB threshold values test

This test is used to designate all the pixels which can be classified to the snow class from the investigated scene at the given time by choosing the threshold values for

every RGB band. The procedure is able to separate snow from bare ground and clouds however it has difficulty in differentiating snow covered ground from special ice clouds

1.4.3. Removing cloud contamination

Pixels that are not classified as cloudy using the previously outlined method are checked for the presence of snow by using the following tests:

1.4.3.1. Standard deviation classification test

At each pixel we used five consecutive RGB images to calculate the standard deviation for every RGB band. When a pixel has a high value in one or more of the RGB standard deviation image, most clouds are detected. This concerns not only undetected ice clouds, but also many other clouds.

1.4.3.2. Residual Cirrus clouds removal test

Using the thermal difference between WV7.3 and IR10.8 we were also able to detect cloudy areas, particularly ice clouds. The radiation emitted at the water vapor channel 7.3 by the surface or low clouds is absorbed by atmospheric water vapor and is not detected by satellites. On the other hand, absorption by atmospheric gases at 10.8 μm is weak, and therefore, detected radiation at 10.8 μm originates mainly from the surface.

1.4.3.3. Temporal classification test

The principle of this test is: if a pixel is classified as snow in one image but not in two neighbor images it is considered to be cloud.

1.4.3.4. Spatial consistency test

This test reclassifies to cloud any snow pixel that is surrounded by five cloud pixels.

1.4.4. Snow composite product method

The last step in the snow cover algorithm is to produce daily composite snow cover map using all available single scene snow cover maps obtained during one day. This reduces the effect of clouds obscuring the surface and further reduces the risk of misclassification of snow pixels.

1.5. Preliminary Results and Discussions

The enhanced capabilities of Meteosat-8 regarding the high spectral and temporal resolution allow a new approach in terms of snow detection. They are used to improve the discrimination between snow and ice clouds, which have partly overlapping spectral signatures and can be difficult to distinguish with spectral information alone.

A preliminary snow detection scheme has been developed in order to improve the snow scene identification using IDL language.

The method was applied to 1126 Meteosat-8 images, from the period 12 March 2007 to 10 April 2007, collected during the day from FMI satellite receiving station.

The Meteosat-8 RGB139i combination (VIS0.6, NIR1.6, IR10.8) (Figure 1) that makes use of 3 different channels was used for identification of the snow areas, especially when viewed as animation.

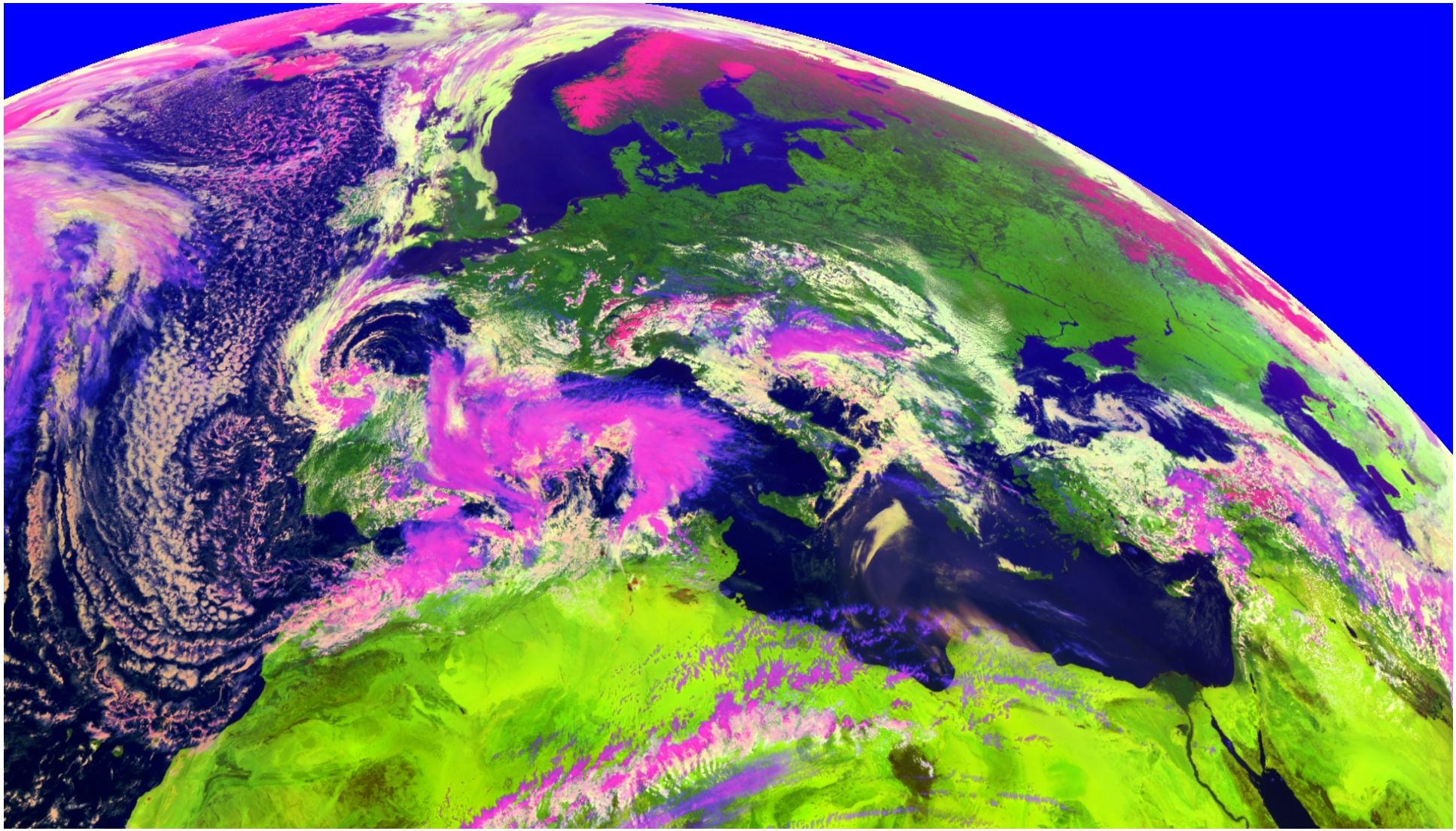

Fig.1. The figure shows a MSG1/SEVIRI image of March 28, 2007, 12:00 GMT as a RGB 139i composite image.

A thresholds test was established for every RGB band in order to delineate snow visible areas from the investigated scenes. Using this test we could separate the snow pixels from many other pixels classes (clouds, free-cloud area, water, etc), but there are still areas of cloud contamination on the snow map (Figure 2).

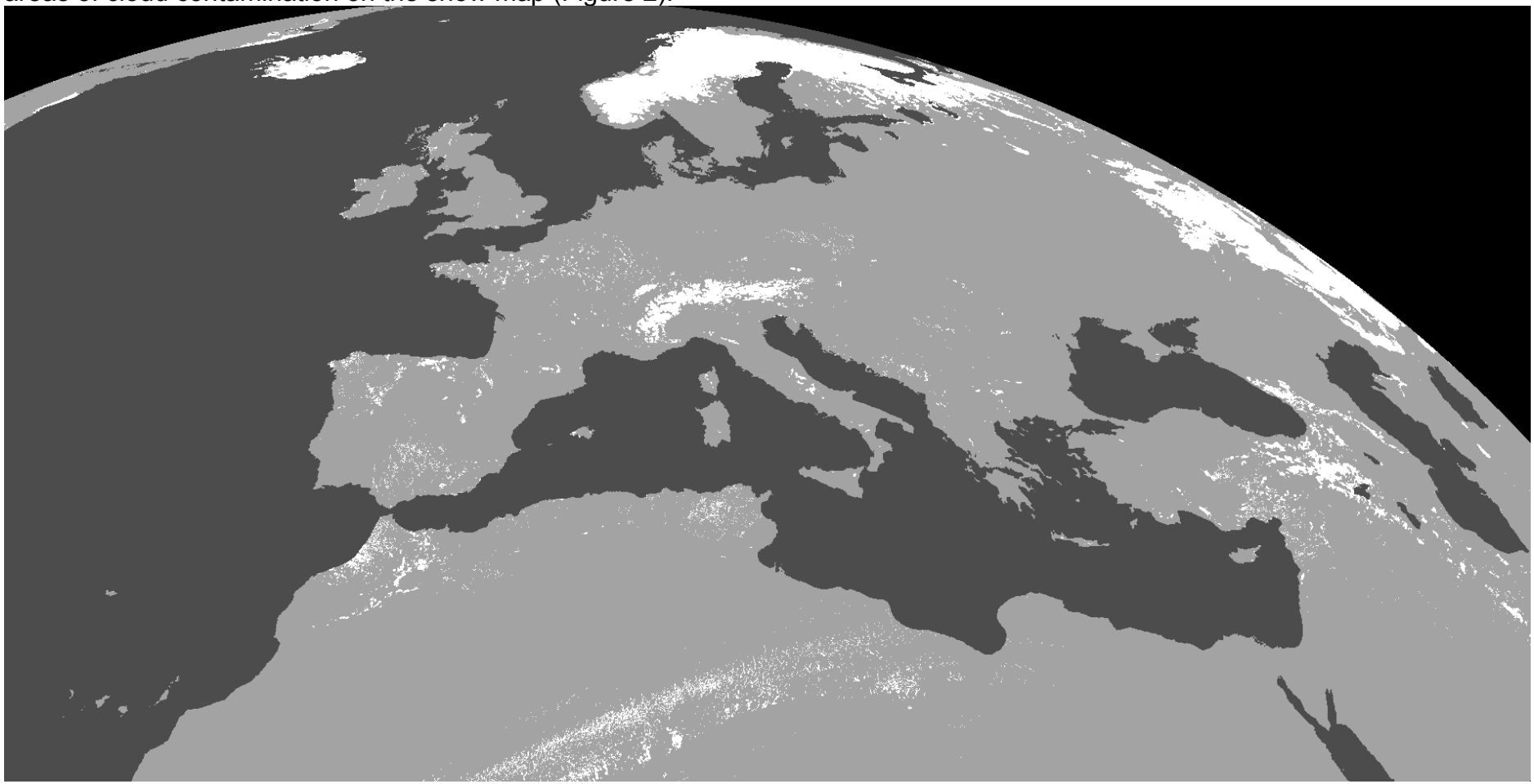

Fig 2. A snow composite map of March 28, 2007 obtained after the RGB threshold test was applied.

For removing the residual cloud we applied four other tests. The standard deviation classification test removes most of cloud areas from snow product obtained with the previous test, but some “thick cirrus pixels” are still classified as “snow pixels”. The rationale behind this test is that most clouds display a more variable behavior in time than the surface. This was demonstrated by De Ruyter de Wildt et al. in [3]. At each pixel, this behavior was quantified by computing the standard deviation of a short time series of pixel values (5 consecutive time steps) Inclusion of this test improves the result. A visual comparison between the RGB image animation and the results obtained with this test reveals that there are no more cloud pixels misclassified as snow.

To remove the residual thick cirrus, we used two SEVIRI channels situated in the infrared part of the spectrum (7.3 and 10.8 μm). The 7.3 μm channel corresponds to one of those “water vapor absorption bands”. Here we are dealing with Earth/atmosphere emissions only. The 10.8 micron channel is in a so-called “clean window” region, in the sense that water vapor and other gases are mostly transparent to radiation having this wavelength, so from a satellite point of view we can in principle see all the way down through the intervening atmosphere to the surface in this band, if a cloud is not in the way. The difference between the two channels is used like a filter to delineate the cloud free areas from cloud areas and it was also revealed in [10].

Raising the threshold value of this difference removed almost all the residual clouds found on the investigated scene but it also reclassified some snow pixels to the cloud class. This test has a tendency to underestimate the snow covered area delineated by the former tests, especially when the snow pixels are covered by clouds during most of the day.

The temporal classification and spatial consistency tests mainly remove cloud pixels which often belong to cloud edges. Using the temporal classification there is also a probability of removing some snow pixels which if, in two neighbor images they were classified as clouds but the high temporal frequency of SEVIRI offers the possibility to snow pixels to be chosen in the snow composition product during the day.

Using all the tests mentioned above, each RGB image is classified and thus instantaneous snow products are obtained. Then they are combined into a composite map. Taking into consideration the tendency of the residual Cirrus cloud removal test to underestimate the snow cover, all the tests described were applied again to the images by using a lower set of threshold values. By statistical comparison between the snow composition product obtained using high test threshold values and the snow composition product given by the low threshold values, other snow pixels are added to the final snow map (Figure 3.).

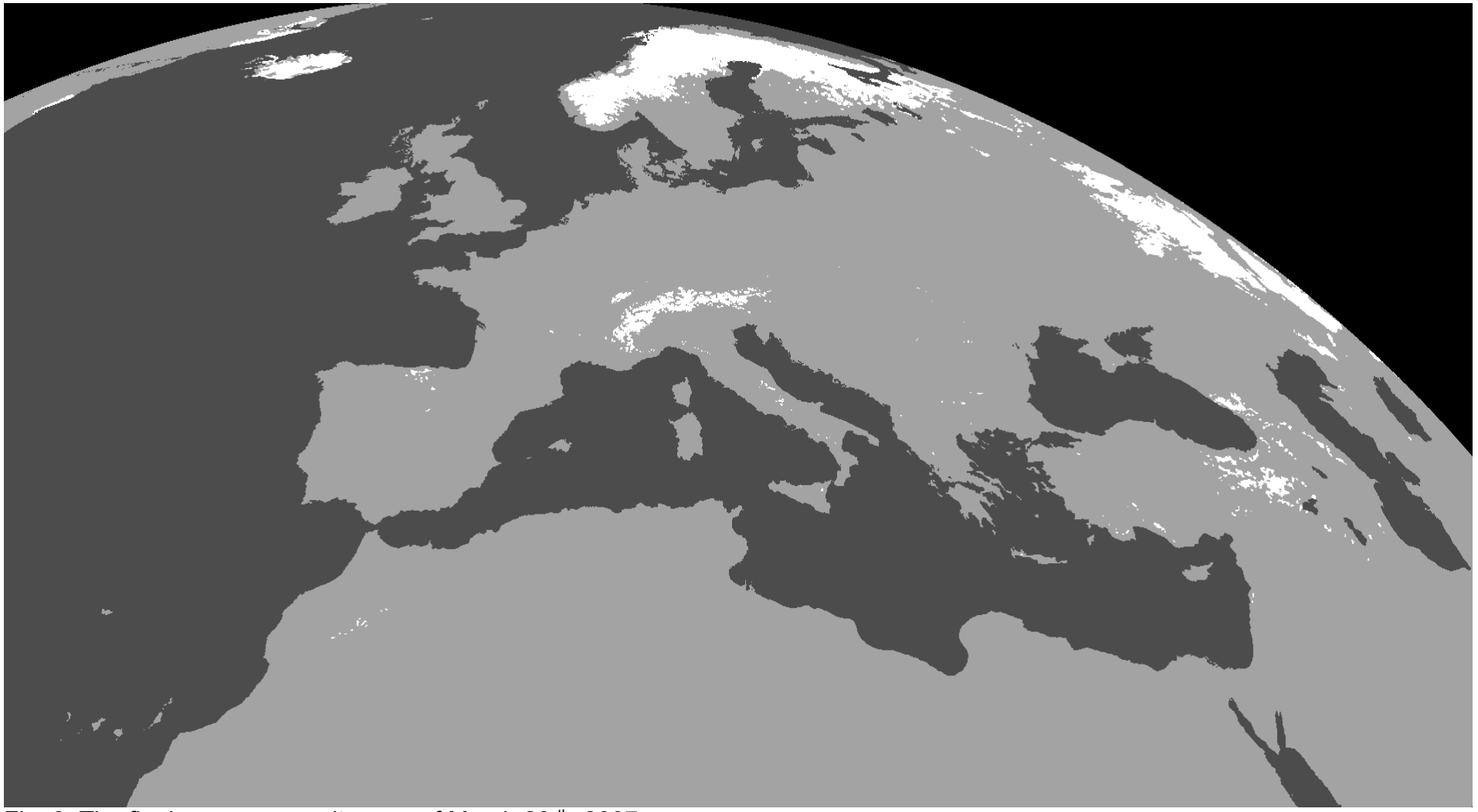

Fig. 3. The final snow composite map of March 28 th, 2007

Section 2

2. RGBHRV139i (HRV+VIS0.6, HRV+NIR1.6, IR10.8i) snow cover algorithm

2.1. Overview

In the previous section the results of preliminary algorithm shows a tendency to underestimate the snow cover area a bit, but it is considerably good in discriminating snow and clouds and mainly because of RGB tools. This helps the viewer to identify the main input signal into image. Based on this result, the work has been extended to develop a new algorithm by adding MSG HRV channel to the visible channels VIS 0.6 and NIR1.6 from the previous combination and by using other tests to discriminate snow and clouds.

2.2. Source of data

The low resolution satellite data (MSG VIS0.6, NIR1.6, IR10.8) used in this algorithm are the same with those used into the preliminary methods. In addition HRV channel has been used for the same dates. All of them were provided through the LRIT/HRIT-Kongsberg receiving station installed at FMI.

2.3. Study Area

Taking account of MSG HRV North sector movement during the day, the area of the study is the common area established for every day between H-SAF project interest region and HRV images.

2.4. Method

The main steps of the new algorithm are:

- RGB HRV139i (HRV+VIS0.6, HRV+NIR1.6, IR10.8) composition images method
- Snow pixel detection using the RGB dynamically threshold values
- A temporal classification test
- Snow map composite product method

2.4.1. RGB HRV139i (HRV+VIS0.6, HRV+NIR1.6, IR10.8i) composite images method.

RGB HRV139i images are composite images generated by combining VIS0.6 and NIR1.6 with HRV channels and then re-create the final RGB images. In order to do this the visible channels, (VIS0.6 and NIR 1.6) and the infrared channel (IR 10.8) are re-sampled to high spatial resolution of channel 12 (HRV). To the eye the resulting images retain the higher resolution of the HRV channel, but at the same time this combination can then highlight different physical features through the differing amounts of red, green and blue and hence give a unique colour to that feature. In our case snow covered ground is pink to dark magenta like in the previous combination.

In order to obtain these RGB images, the main tasks of this method consist of the following:

1. Processing VIS0.6, NIR1.6, IR10.8 satellite data
   This step was described in the section 1 of this report.
2. Processing HRV data
   2.1. Geometric Coding

Documentation to implement this step is provided by EUMETSAT in [12]

2.2.Solar zenith angle calculations

Documentation to implement this step is provided by EUMETSAT in [5]

2.3 Radiometric Calibration

The radiometric conversion procedure was compiled from the EUMETSAT website [8]

3. Re-sampled VIS0.6, NIR1.6, IR10.8 satellite data
   This task consists of re-sampled to the spatially higher resolution of channel 12 (HRV).
4. RGB HRV139i combination images product

All the processing stages were written in the IDL language and run on the FMI server.

2.4.2. RGB dynamic threshold test

In order to discriminate snow from others features of image scene dynamic thresholds have been implemented into new algorithm. Their values have been adapted to the geographical regions and acquisition time of satellites images.

2.4.3. Temporal classification test

A pixel is classified as snow, if in two neighboring images it is considered to be snow

2.4.4. Snow map composite product method

The daily composite snow cover map is done by using all available single scene snow cover maps obtained for that specific day. This reduces the effect of clouds obscuring the surface and further reduces the risk of misclassification of snow pixels**.** A cloud mask was created and added to the snow cover maps. The cloud mask is done using threshold tests to RGB bands.

2.5. Results and discussions

For snow cover detection over HSAF geographical area, a new algorithm has been created by adding spectral information of MSG HRV channel to the visible channels VIS0.6 and NIR1.6. It is more easy to distinguish snow and ice using this RGB combination, particularly if there are no clouds around to confuse the issue than using the previous combination. Snow cover maps have more details about snow areas and they have a more dendritic pattern over mountain regions (Figure 4).

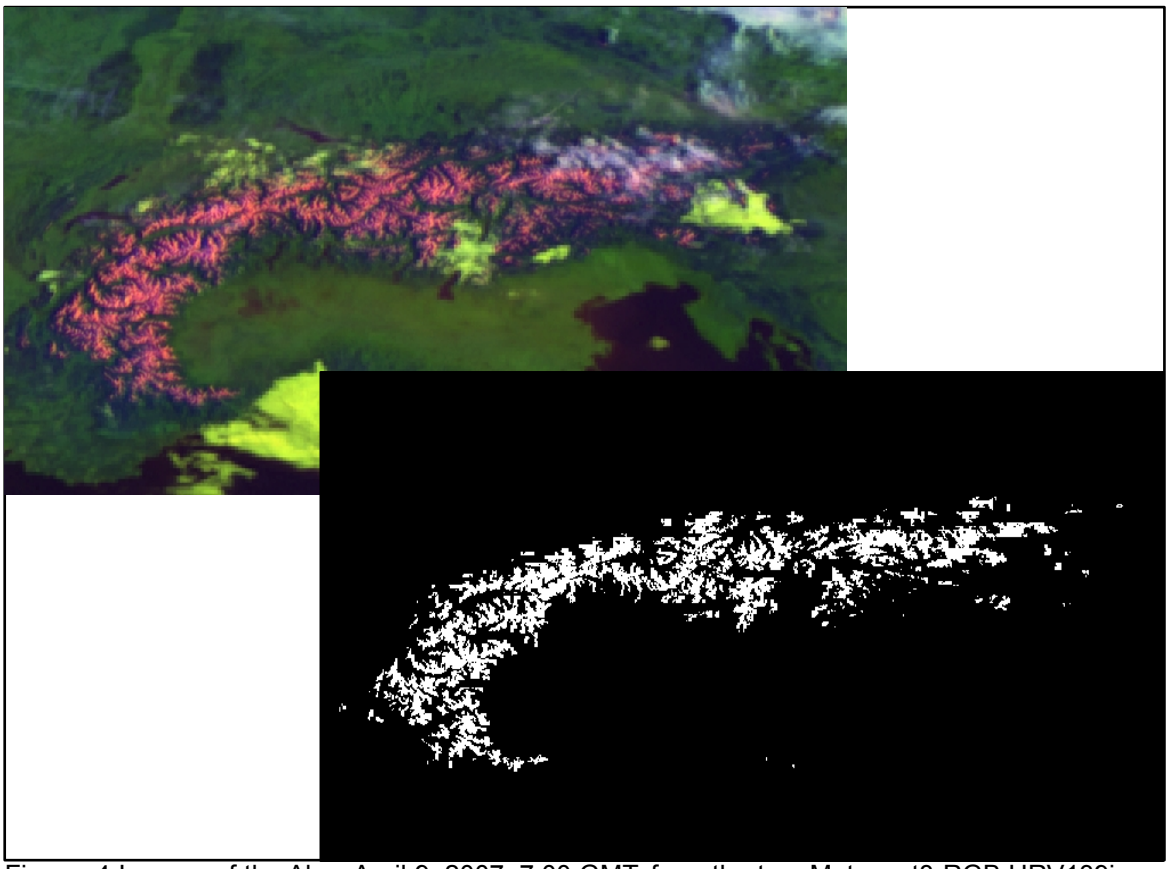

Figure. 4 Images of the Alps, April 9, 2007, 7:00 GMT, from the top, Meteosat8-RGB HRV139i, and instantaneous snow cover map obtained before clouds removing test were applied into new algorithm.

Another example is shown in figure 5 where snow covered ground is delineated over Turkey.

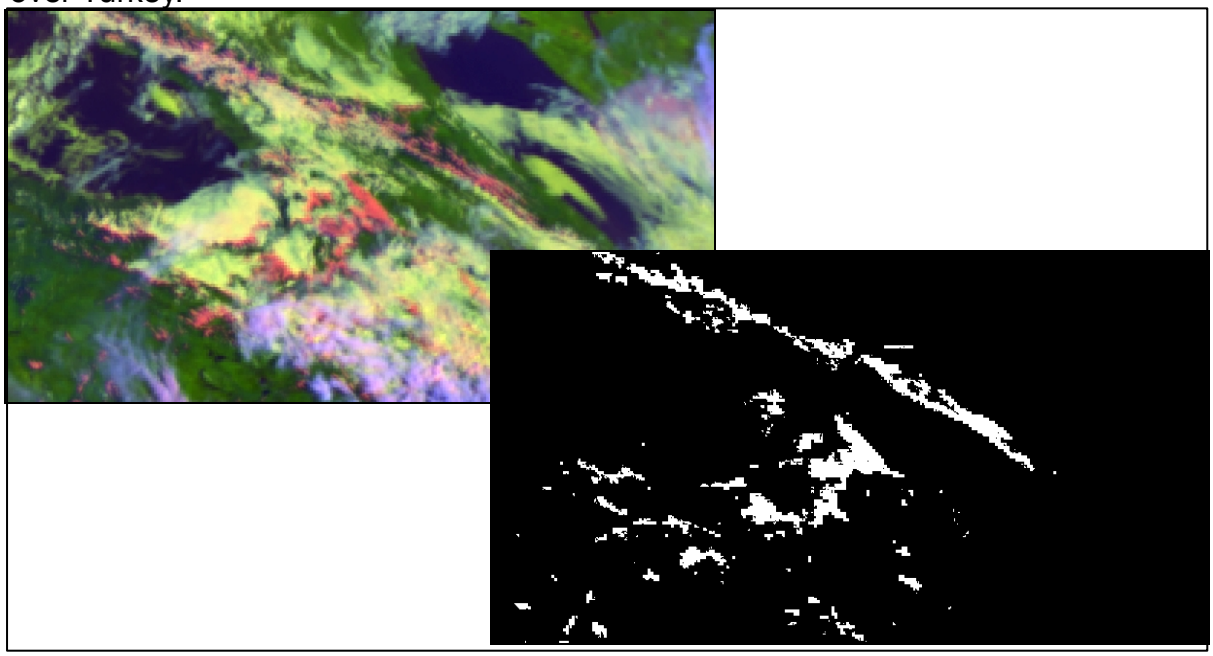

Figure. 5 Images of the Turkey, April 9, 2007, 7:00 GMT, from the top, Meteosat8-RGB HRV139i, and instantaneous snow cover map obtained before clouds removing test were applied into new algorithm.

Also in the forested areas, this new combination offers more details about snow covered ground. In this representation snow shows up in shades of dark pink – magenta. The new algorithm has mapped more snow pixels than the previous and has capability to discriminate much better snow areas from others, particularly cloud areas (example figure 6).

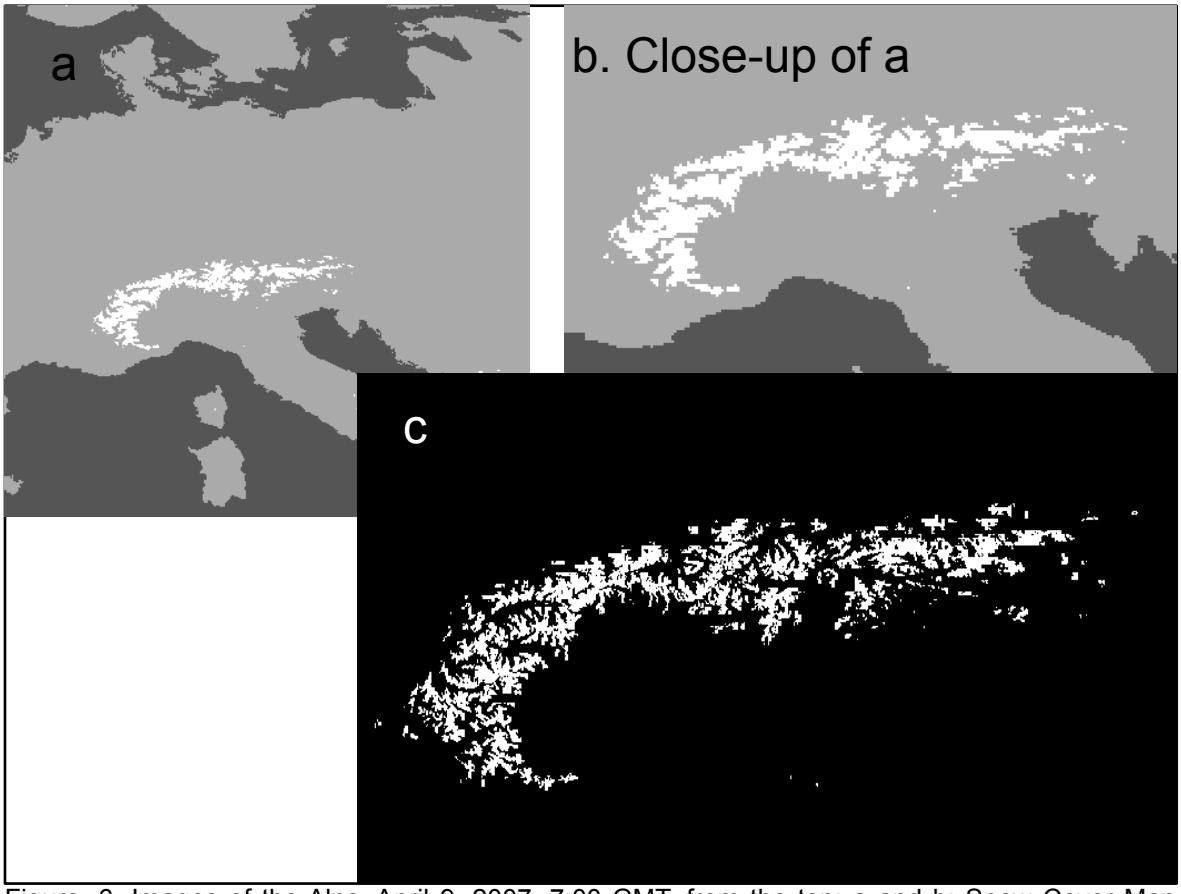

Figure. 6. Images of the Alps, April 9, 2007, 7:00 GMT, from the top: a and b: Snow Cover Map (previous algorithm); c: instantaneous snow cover map obtained before clouds removing test were applied (new algorithm)

The results obtained from a comparison between new and previous algorithms show good performances. The improvement compared to first results given by preliminary algorithm is remarkable.

Section 3

3. Comparison of RGBHRV139i snow products with the baseline HSAF snow recognition and LSA SAF snow cover (development version) products.

The snow maps compared in this report were produced using three different methods and are the following:

3.1. RGBHRV139i Snow Cover Composite Maps.

The RGB HRV139i Snow Cover Maps algorithm was described in the section 2 of this report. The classification of RGBHRV139i Snow Cover Maps consists of the following three different classes: snow, clouds, water. The land/ water mask is provided by FMI. It is the same with HSAF land/water mask.

3.2. HSAF Snow Cover Composite Maps

Detailed description of HSAF Snow Maps Product Algorithm and land/water mask are provided by [2]
Every pixel of HSAF snow cover maps is classified into one of the following classes: snow, clouds, water.

3.3. LSA SAF (development version) Snow Composite Maps

In this study the results of LSA SAF Algorithm Version 2.03 is used. This is a new version developed by FMI.
The study area and land/water mask used are described by LSA SAF in [9].
The resulting snow cover map produced from LSASAF (development version) Snow Algorithm contains a classification of each pixel into one of the following classes: totally snow covered, partially snow covered, land, unclassified, water.

RGBHRV139i snow cover maps were compared with HSAF snow cover maps for 27 days between March 12, 2007 and April 10, 2007. RGBHRV139 snow cover maps were also compared with LSA SAF (development version) snow maps. In the last case, comparisons were made for 4 days of the same period (March 13, March 21, March 28 and April 1).

3.4. Methods

3.4.1. Re-classification

In order to compare the snow cover maps, the daily snow composite maps from the different sources are pre-processed into similar format. In their original files the HSAF snow maps and LSAF SAF snow maps have their own classification code of product. The classification is translated into a common classification at the pre-processing using the same code.

3.4.2. Resampling

The others two snow maps were resampled to the RGB HRV139 snow map resolution.

3.4.3. Map comparison

With each pair of snow composite maps in the same resolution, the same area, the same code of classification, a comparison map was created. All the categories were compared, except water class and space class when the comparison is done between RGB HRV139 snow maps and HSAF snow maps and also pixels of space class for comparison RGB HRV139 snow maps with LSA SAF snow maps. The comparisons were done to evaluate the agreement and disagreement within different class pairs obtained. For each pair of snow maps compared, an image was produced indicating the type of agreement or disagreement for each pixel. These images were summarized to determine the information of the percent overall agreement. The overall accuracy is defined as the sum of correctly classified pixel groups divided by the total number of pixels. The following groups are considered snow/snow, cloud/cloud, land/ land and for RGBHRV139i-HSAF and for RGBHRV139i-LSA SAF the overall accuracy was performed taking account of the following correctly classified pixels groups:

1. snow/snow, cloud/cloud, land/land, water/water
2. snow/snow, snow/partially snow, cloud/cloud, land/land, water/water.

3.5.Results and discussions

3.5.1. RGB HRV139i – HSAF Snow Map Comparison

The table 1 presents the average agreement and disagreement of RGBHRV139i snow maps with the HSAF snow maps.

Date	Snow/Snow	Snow/Clouds	Snow/Land	Clouds/Snow	Clouds/Clouds	Clouds/Land	Land/Snow	Land/Couds	Land/Land	Overall Acc.
2007.03.12	72.8	5.5	0.8	22.1	87.4	6.9	5.0	7.1	92.3	89.9
2007.03.13	80.9	4.0	0.8	16.1	87.8	8.6	3.1	8.2	90.6	89.3
2007.03.14	76.6	4.0	0.8	21.1	89.7	13.8	2.3	6.2	85.5	86.1
2007.03.15	**83.7**	**5.3**	**0.8**	**14.7**	**89.1**	**10.6**	**1.6**	**5.7**	**88.6**	**88.5**
2007.03.19	56.2	4.0	0.3	37.9	92.5	7.2	6.0	3.5	92.6	**90.9**
2007.03.20	74.9	3.6	0.8	18.8	87.0	10.7	6.4	9.4	88.5	87.1
2007.03.21	74.6	3.5	1.3	21.2	92.8	26.7	4.2	3.7	72.0	81.0
2007.03.22	63.2	2.6	1.6	35.1	94.1	29.5	1.7	3.3	68.9	79.3
2007.03.23	73.6	3.8	1.9	22.9	91.8	14.7	3.5	4.4	83.5	86.6
2007.03.24	67.9	3.2	1.2	30.7	93.3	10.0	1.4	3.5	88.8	89.0
2007.03.25	68.5	3.3	1.4	30.8	91.4	16.5	0.7	5.4	82.1	83.6
2007.03.26	62.8	3.7	2.1	33.9	88.5	10.8	3.3	7.8	87.2	85.7
2007.03.27	76.5	4.2	1.4	19.8	86.4	12.4	3.7	9.4	86.1	85.5
2007.03.28	71.4	3.7	2.1	24.0	89.0	15.8	4.6	7.3	82.2	83.0
2007.03.29	69.5	1.9	2.3	28.5	93.3	18.6	2.0	4.8	79.1	81.9
2007.03.30	67.1	2.3	1.5	26.0	92.7	13.7	6.9	5.1	84.8	85.4
2007.03.31	63.0	2.4	0.7	31.7	90.2	19.2	5.3	7.4	80.1	82.0
2007.04.01	53.1	2.6	0.8	42.4	92.1	18.7	4.4	5.2	80.5	82.9
2007.04.02	57.6	2.6	0.5	34.0	93.9	26.7	8.4	3.5	72.8	**78.9**
2007.04.03	48.5	2.3	0.4	44.2	94.5	24.3	7.3	3.2	75.3	79.6
2007.04.04	**44.2**	**2.2**	**0.3**	**54.9**	**96.0**	**18.8**	**0.9**	**1.8**	**80.9**	**83.5**
2007.04.05	58.4	2.3	0.7	35.7	89.3	16.0	5.9	8.3	83.3	84.2
2007.04.06	55.3	1.3	0.7	42.7	95.0	18.5	2.0	3.7	80.9	85.0
2007.04.07	58.7	1.9	0.6	38.6	94.5	16.4	2.7	3.6	83.0	85.7
2007.04.08	48.4	2.4	0.5	50.6	91.6	18.7	1.0	6.1	80.8	82.2
2007.04.09	51.1	3.0	0.6	45.8	92.2	15.7	3.1	4.9	83.8	83.9
2007.04.10	59.6	2.5	0.8	38.7	93.1	16.5	1.8	4.4	82.7	84.6
AVERAGE	**64.4**	**3.1**	**1.0**	**31.9**	**91.5**	**16.1**	**3.7**	**5.4**	**82.8**	**84.6**

Table 1. Summary of comparisons between RGB HRV129i /HSAF snow cover Maps showing agreement and individual disagreements between different classes. The values are given by percent (%).

A comparison of RGB snow maps and HSAF reveals a good overall agreement over the entire study period with an average of overall accuracy of 84.6 % for the snow, clouds, land classes. The daily overall accuracy for the study period ranges from accuracies of 78.9 % to almost 91% for 27 selected days over HSAF study area, even the agreement between snow classes from both maps are not so high. This overall accuracy is given by high agreement values of others two groups: clouds/clouds (91.5% average) and land/land (82.8 % average). These snow cover algorithms share the same land-water mask.

The agreement of snow classes between the two maps mentioned has a medium value (average 64.4%). The daily agreement value of snow/snow group ranges from 44.2 % to almost 84% and the percent values of cloud/snow disagreement corresponding to snow/snow group values mentioned are 54.9% and respective 14.7%. These values represent the higher and lower value of clouds/snow group for 27 selected days over HSAF study area. The percent disagreement values of others groups corresponding to higher and lower values of snow/snow group are not the lower respective the higher for respective groups. The cloud cover classification can be considered to be the main reason for the relatively low classification accuracies for snow/snow group. The average value of clouds/snow group disagreement is relatively high, almost 32%, which indicates RGBHRV139i snow cover algorithm classifies some HSAF snow pixels as clouds class. The percent value of clouds/snow group depend on how much the satellite image scene has clouds, especially ice clouds, where HSAF algorithm has a tendency to classify them as snow class. A typical case is when snow cover area is obscured by clouds most of the day and HSAF snow cover maps has a tendency to classify these pixels as snow class.

For cloud free areas the agreement between the two snow cover maps are usually good, RGBHRV139i algorithm works as well or better than HSAF algorithm because of HRV channel implementation in a RGB algorithm. The percent average value of snow/land group disagreement is 3.1% and the daily disagreement value of snow/land group ranges from 0.3 % to 2.3 %. The RGBHRV139i /HSAF comparisons show that RGBHRV139i snow algorithm have found more snow in forested areas than HSAF snow cover algorithm has done during cloud free days for these areas. The largest disagreement for this group occur at the end of March and it is starting on March 21 until on March 28 when forest areas are not obscured by clouds (example Finland region).An other source for this disagreement is caused by possible mis-colocation of HRV channel to the other channels (VIS0.6, NIR1.6, IR10.8), and this could be detectable at the edge of HSAF snow cover areas, but it cant be more than one pixel on both directions x, y. Another explanation of these differences specially in forested areas could be the snowmelt period. Given the high resolution of the HRV channel, RGBHRV139i snow algorithm has the possibility to discriminate much better partially snow pixels than HSAF snow algorithm.
Figures 7, 8, 9, and 10 show subsets of the comparison for April 1, 2007. It can be seen in comparisons, that when cloud cover is prevalent in an image, the HSAF snow product can sometimes misinterpret the cloud cover as either ice or snow.

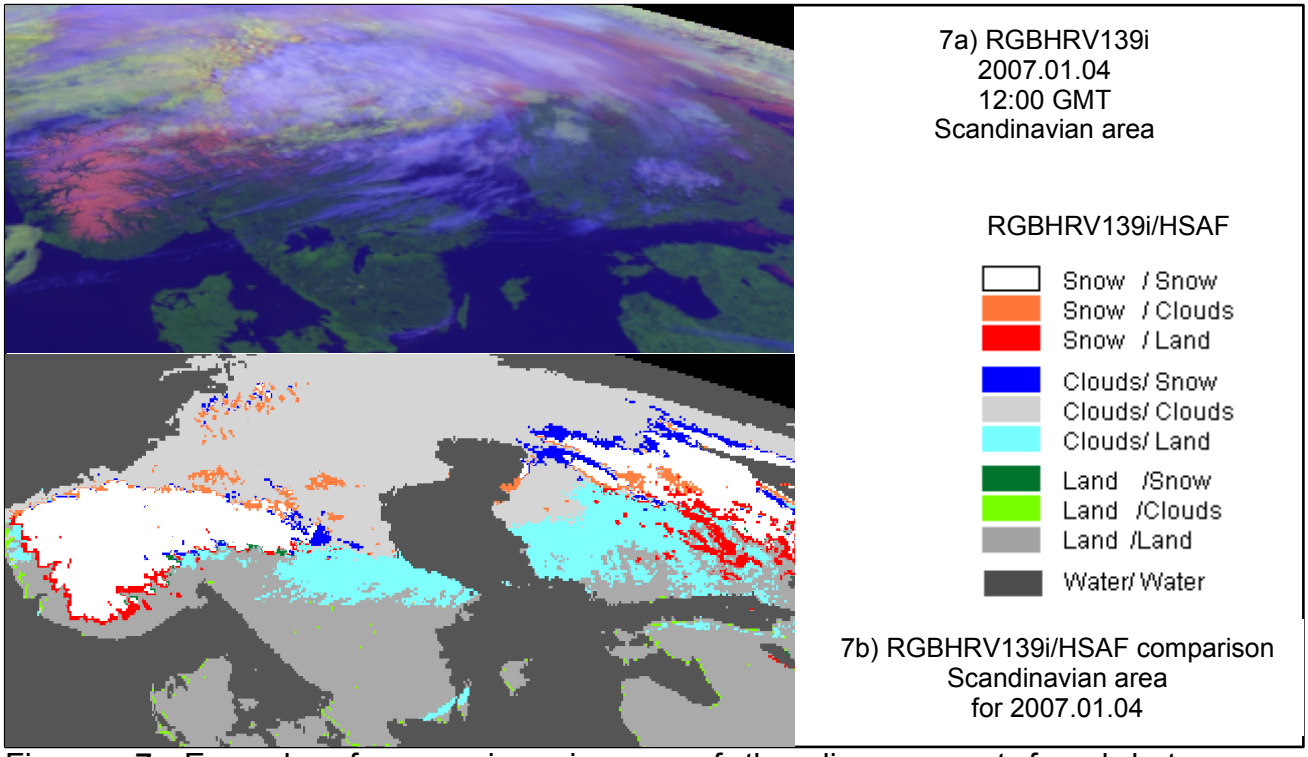

Figures 7. Example of comparison images of the disagreement found between RGBHRV139i snow cover map and HSAF snow cover map.

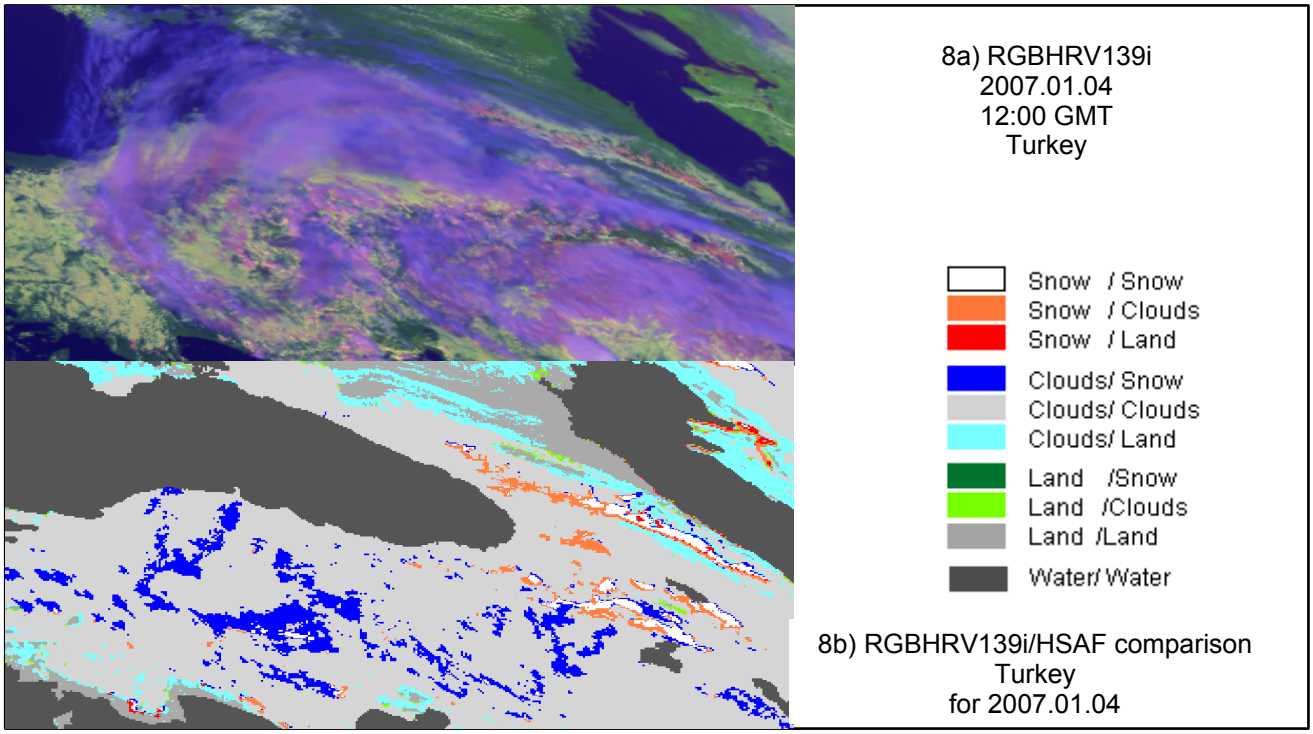

Figure 8. Example of comparison images of the disagreement found between RGBHRV139i snow cover map and HSAF snow cover map.

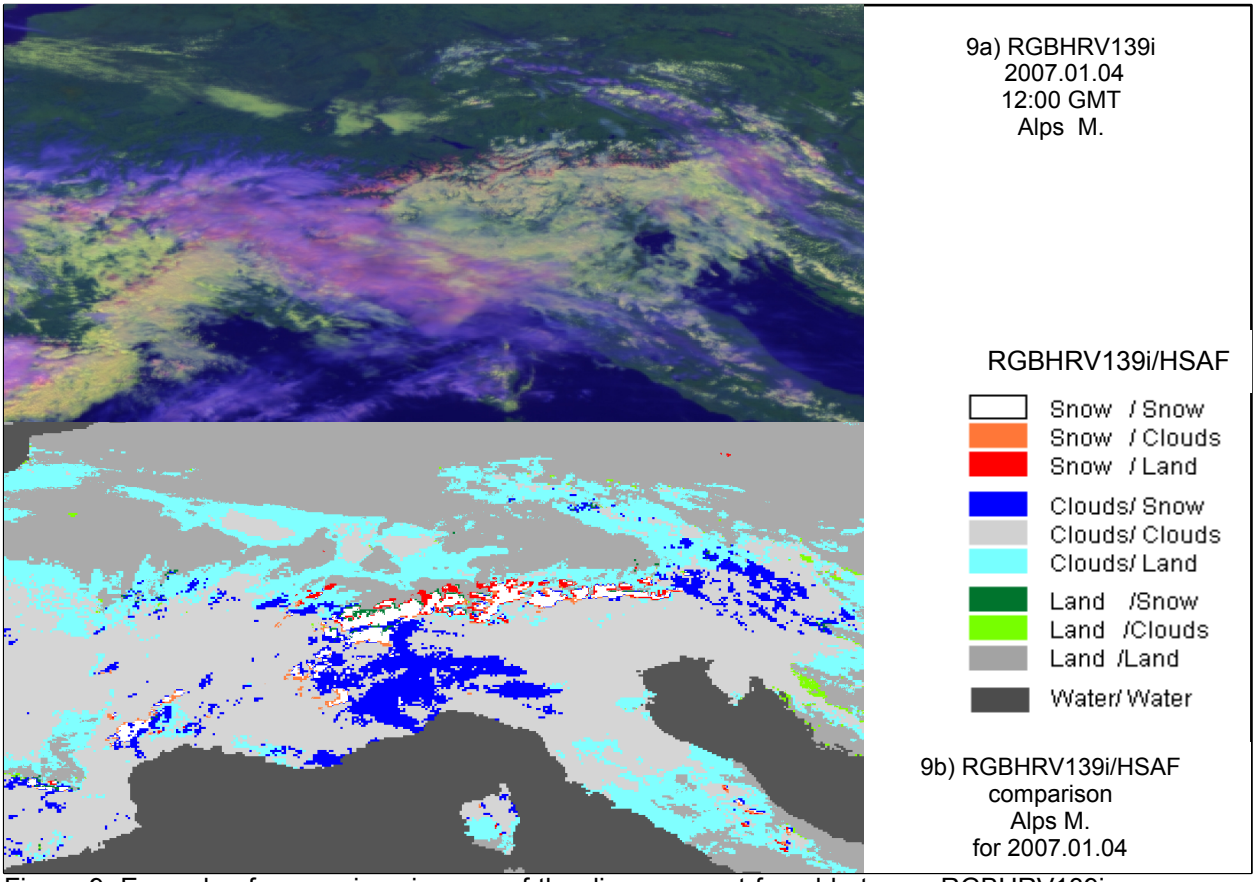

Figure 9. Example of comparison images of the disagreement found between RGBHRV139i snow cover map and HSAF snow cover map.

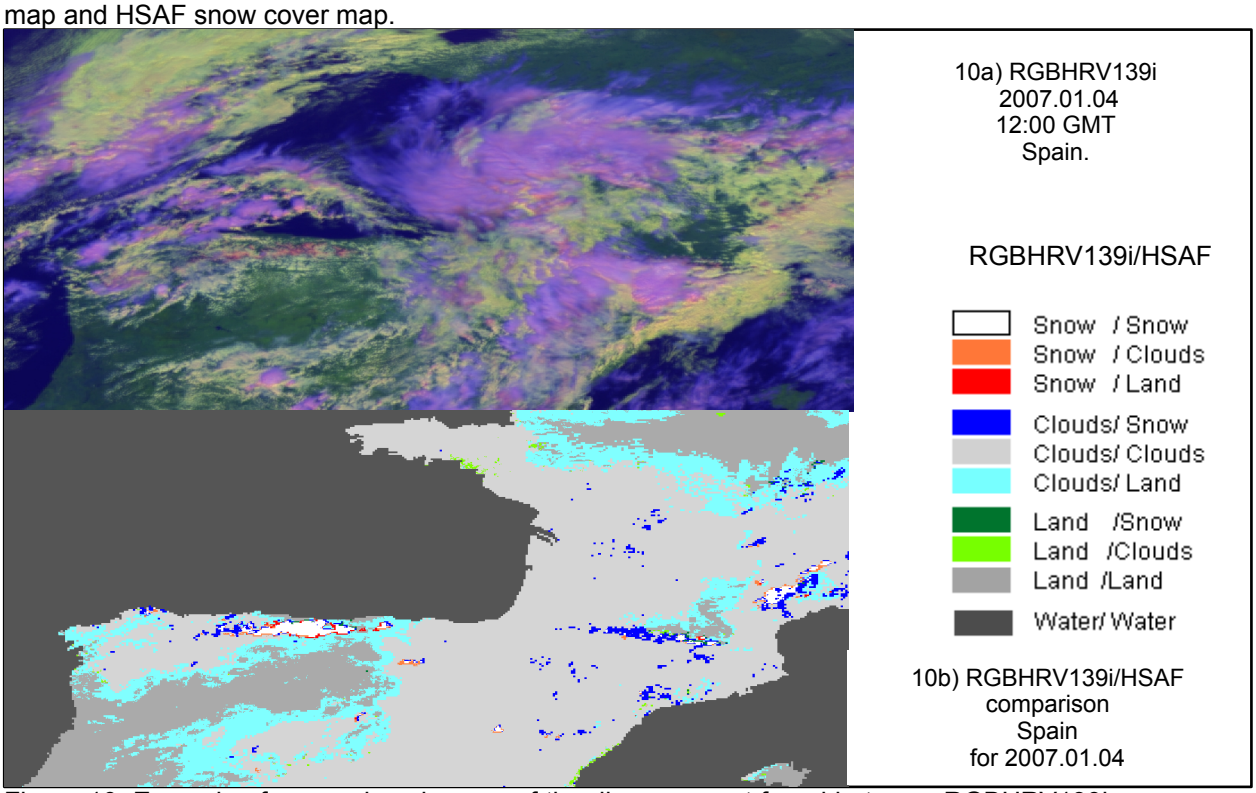

Figure 10. Example of comparison images of the disagreement found between RGBHRV139i snow cover map and HSAF snow cover map.

3.5.2. RGB HRV139 – LSA SAF Snow Map Comparison

The comparisons between RGBHRV139i snow cover maps and LSA SAF snow cover maps (development version) show more closed results (Table 2).

Date	Snow/Snow	Snow/P.Snow	Snow/Unclassified	Snow/Land	Snow/Water
2007.03.13	83.6	38.0	19.0	1.6	0.7
2007.03.21	89.0	77.1	11.2	2.3	1.0
2007.03.28	82.5	32.9	14.4	1.1	1.2
2007.04.01	68.1	32.8	10.1	0.9	0.5
Average	**80.8**	**45.2**	**13.7**	**1.5**	**0.8**
Date	**Clouds/Snow**	**Clouds/P.Snow**	**Clouds/Unclassified**	**Clouds/Land**	**Clouds/Water**
2007.03.13	4.2	36.2	76.2	38.9	2.5
2007.03.21	3.6	15.4	86.2	50.3	2.7
2007.03.28	7.5	30.3	81.7	40.0	1.5
2007.04.01	22.7	57.6	87.4	46.6	2.2
Average	**9.5**	**34.9**	**82.9**	**44.0**	**2.2**
Date	**Land/Snow**	**Land/P.Snow**	**Land/Unclassified**	**Land/Land**	**Land/Water**
2007.03.13	8.7	22.1	2.0	56.2	1.7
2007.03.21	5.4	6.8	0.9	43.2	1.1
2007.03.28	7.3	34.3	1.9	55.5	2.2
2007.04.01	6.7	8.2	0.5	49.0	2.2
Average	**7.0**	**17.8**	**1.3**	**51.0**	**1.8**
Date	**Water/Snow**	**Water/P.Snow**	**Water/Unclassified**	**Water/Land**	**Water/Water**
2007.03.13	3.5	3.8	2.8	3.2	95.2
2007.03.21	2.0	0.8	1.7	4.2	95.2
2007.03.28	2.7	2.5	2.0	3.4	95.2
2007.04.01	2.5	1.5	1.9	3.5	95.2
Average	**2.7**	**2.1**	**2.1**	**3.6**	**95.2**

Date	Ov. Acc without P.Snow	Ov. Acc with P.Snow
2007.03.13	75.7	75.8
2007.03.21	75.9	76.0
2007.03.28	75.9	75.9
2007.04.01	73.3	73.4
Average	**75.2**	**75.3**

Table 2 Summary of comparisons between RGB HRV129i /LSAF snow cover maps showing agreement and individual disagreements between different classes. The values are given by percent (%).

For this comparison the RGB HRV139i snow cover maps were adjusted to the LSA SAF study area. The daily overall accuracy ranges from accuracies of almost 73.3 % to76.0

% for 4 selected days over LSA SAF study area. In this case, even if the average overall accuracy values are lower than the average overall accuracy values for RGBHRV139i/HSAF comparison, the average percent agreement value of snow/snow group between the RGBHRV139i snow cover maps and the LSA SAF snow cover maps was better than in the previous comparison. The RGBHRV139i snow cover maps have showed 80.8% average agreement when have compared with LSA SAF snow cover maps. On April 1, 2007 comparison for the snow/snow group has a lower agreement than others days. Mainly, this is given by a low agreement of this group on eastern part of the globe, at high latitudes, longitudes and satellite zenithal angles (above 73^0 values), possible on the forested areas.

Table 3 summarizes also the variability of the RGBHRV139i snow cover performance versus LSAF snow cover performance. For 4 selected days the agreements of snow/snow group are largest on March days with a peak on March 21, 2007 and with a low value on April1 2007. It is likely that these agreements are related with cloud cover on forested area (example, Finland region) and with the snow melt period. On March13 and 28, the disagreements of land/partially snow group are 22.1 % respective, 34.3 % and the forested areas are almost cloud free areas during these days.
The agreement of snow/snow group has diminished as the percent of snow pack into pixel has diminished also.

Figures 11, 12, 13 and14 shows subsets of the comparison map for April 1:

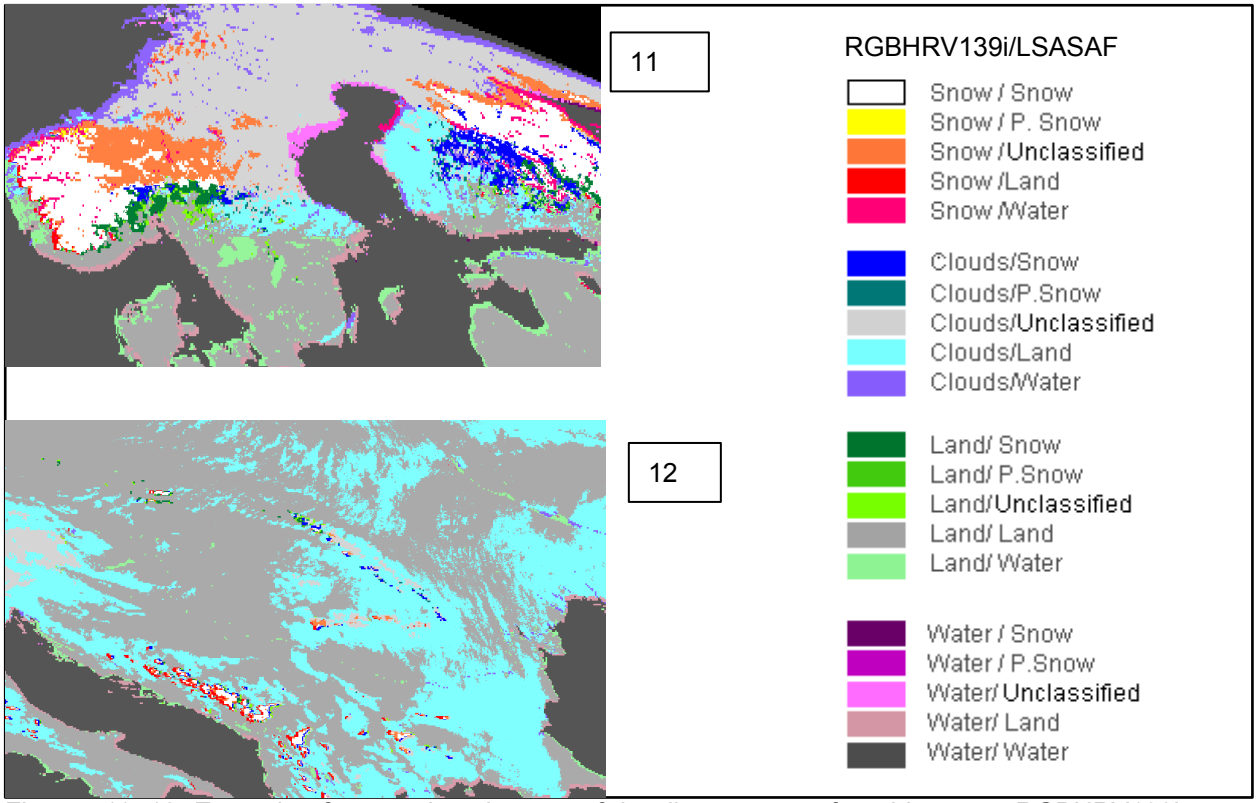

Figures 11, 12. Example of comparison images of the disagreement found between RGBHRV139i snow cover map and LSASAF snow cover map, April 1, 2007, Scandinavia Area (11.), Romania (12).

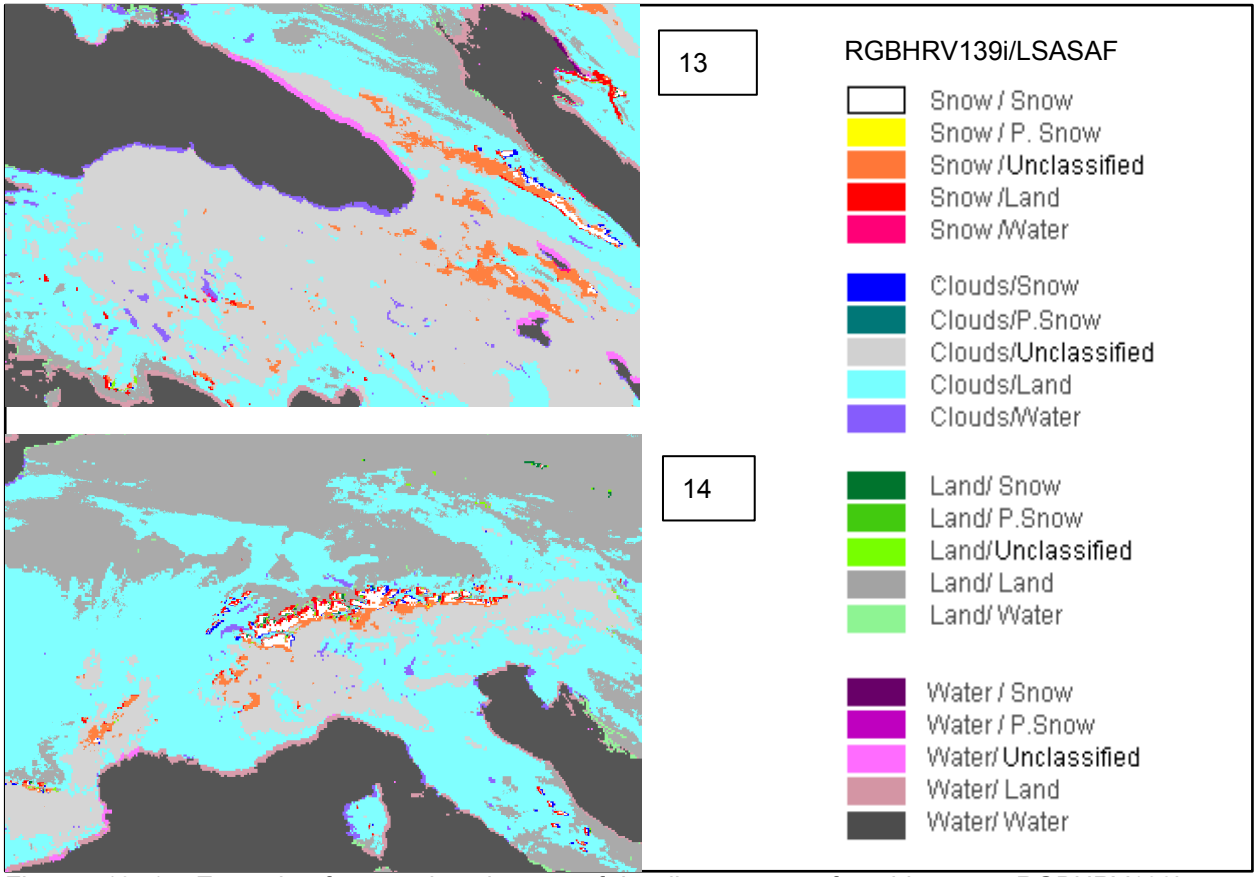

Figures 13, 14. Example of comparison images of the disagreement found between RGBHRV139i snow cover map and LSASAF snow cover map, April 1, 2007, Alps M (14.), Turkey (13).

The LSAF snow cover maps (development version) has one more class compared to the other two: partially snow covered class. In terms of average value, in this case only 45.2 % of pixels are mapped as snow by RGB HRV139i snow cover algorithm.

The RGB HRV139i snow cover algorithm has found almost 14 % of snow pixels from unclassified category of LSA SAF snow cover maps.

As in the previous comparison for cloud free areas with full snow pixel, the agreement between the two snow cover maps are usually good, RGBHRV139i algorithm works as well or better than LSAF SAF algorithm because of HRV channel implementation in a RGB algorithm.
For others groups, this comparison is difficult because of the different land-water mask. Most of the disagreement can be explained by the difference of land-water masks used, the land /water mask from LSAF snow cover maps

Conclusions

In section 1, a preliminary snow detection algorithm has developed using Meteosat8 RGB139i image in order to improve the snow scene identification.
A suite of tests has been implemented into it to derive snow cover maps and to produce a daily composite snow maps. The processing stages have been written using the IDL language and have run on the FMI server.

A static threshold values test have been applied to the RGB139i bands in order to discriminate ice cloud class from snow class because usually RGB composition images have the capability to retain the qualitative signal of the targets, in our case from snow covered surface and from clouds.
The standard deviation test applied to the snow product obtained with the previous test usually separates well snow from the other classes, especially ice cloud.
Residual Cirrus clouds have been removed by employing a test based on the thermal difference between WV7.3 and IR.10.8 channels. This test overestimates the cloud amount but by doing so the pixels classified as snow have had a high accuracy.
A first validation of the preliminary results has been done by visual inspection of the animated RGB139i product.

This preliminary algorithm has a tendency to underestimate the snow cover area a bit, but it is somewhat better in discriminating snow and clouds.

Based on this conclusion a new algorithm has been created by adding MSG HRV channel to the visible channels VIS0.6 and NIR1.6 from the previous combination. This work is described in **section 2**.

The resulting RGBHRV139i images retain the higher resolution of the HRV channel, but at the same time this combination can then highlight different physical features on image scene than the previous combination.
Other tests to discriminate snow and clouds have been implemented into new algorithm by using dynamic thresholds. Their values have been adapted to the geographical regions and acquisition time of satellites images..

The results obtained from a comparison between new and previous algorithms show good performances. Using this representation with HRV, snow cover maps have more details about snow areas and they have a more dendritic pattern over mountain regions, This algorithm is needed for comparison of the present HSAF baseline and LSA SAF development algorithms**.**

In section 3 two different snow map comparisons have been performed. The first comparison has been done between RGBHRV139i snow cover maps and HSAF snow cover maps. The second comparison is between RGBHRV139i snow cover maps and LSA SAF snow cover maps (development version).
The RGBHRV139i snow cover maps have a tendency to mapping snow better than HSAF snow cover map specially in forested area (i.e., Finland) but less than LSA SAF snow cover map for the same area.

Also for both comparisons, there are differences at the edges of snow pack, in mountain region, given by capabilities of HRV channel, RGBHRV139i snow cover algorithm mapped more snow than others. Inter-comparison of snow maps is problematic because it is difficult to determine which map is more accurate, but it provides a lot of information on the viability and limitations of different snow mapping methods.

Future work

The plan in Cluster 3 of HSAF is to validate the results of these methods with in situ data. For this purpose there will be a joint experiment with LSA SAF, CLA SAF and HSAF, **SNO**w **R**eflectance **T**ransition **EX**periment (SNORTEX) in winter/spring 2008.

References

1. Allen, R. C., Jr., P. A. Durkee, and C. H. Wash, 1990: Snow/cloud discrimination with multispectral satellite measurements. *J. Appl. Meteor.,* **29,** 994–1004.

2. Algorithms Theoretical Definition Document. ATDD-1.0. Part.4.HSAF/CDR/DOC.ID.

3. De Ruyter de Wildt, M. S., Seiz, G. and Grün, A., 2006. Snow mapping using multi-temporal Meteosat-8 data. *EARSeL eProceedings*, 4(1), 18-31.

4. Gesell, G., 1989: An algorithm for snow and ice detection using AVHRR data: An extension to the APOLLO software package.*Int. J. Remote Sens.,* **10,** 897–905

5. Govaerts, Y and Clerici, M. 2004. Seviri Toolbox (SPT Version 2.4). Doc No: EUM/OPS-MSG/TEN/03/0011. Available at http://www.eumetsat.int/

6. Hall, D. K., G. A. Riggs, and V. V. Salomonson, 1995: Development of methods for mapping global snow cover using Moderate Resolution Imaging Spectroradiometer data. *Remote Sens. Environ.,* **54,** 127–140.

7. Hyvarinen, O., Karlsson, K-G., Dybbroe, A., 1999: Investigations of NOAA AVHRR/3 1.6 mm imagery for snow, cloud and sunglint discrimination, SAFNWC Visiting Scientist Report, Available at http://www.smhi.se/saf under Documents.

8. http://www.eumetsat.int/idcplg?IdcService=GET_FILE&dDocName=pdf_msg_seviri_rad2refl&RevisionSelectionMethod=LatestReleased

9. Product User Manual SNOW COVER , SAF/LAND/FMI/PUM/SC/2.5. Available at http://landsaf.meteo.pt/

10. Mecikalski, J.R., and K.M.Bedka, 2006: Forecasting convective initiation by monitoring the evolution of moving convection in daytime GOES Imagery. Mon. Wea. Rev.134, 49-78

11. MSG Interpretation Guide. Available at http://oiswww.eumetsat.org/WEBOPS/msg_interpretation/index.html

12. MSG Level 1.5 Image Data Format Description, EUM/MSG/ICD/105

13. Romanov, P., Gutman, G., and Csiszar (2000) Automated monitoring of snow cover over North America with multi-spectral satellite data. Journal of Applied Meteorology, 39, pp. 1866-1880.